The Effects of Inhaling Hydrogen Gas on Macrophage Differentiation, Fibrosis and Lung Function in Mice with Bleomycin-induced Lung Injury

Toshiyuki Aokage
Okayama University Graduate School of Medicine
Mizuki Seya
Okayama University Graduate School of Medicine
Takahiro Hirayama
Okayama University Graduate School of Medicine
Tsuyoshi Nojima
Okayama University Graduate School of Medicine
Masumi Iketani
Tokyo Metropolitan Institute of Gerontology
Michiko Ishikawa
Hyogo College of Medicine
Yasuhiro Terasaki
Nippon Medical School
Akihiko Taniguchi
Okayama University Graduate School of Medicine
Nobuaki Miyahara
Okayama University Graduate School of Health Sciences
Atsunori Nakao
Okayama University Graduate School of Medicine
Ikuroh Ohsawa
Tokyo Metropolitan Institute of Gerontology
Hiromichi Naito (✉ naito-hiromichi@s.okayama-u.ac.jp)
Okayama University Graduate School of Medicine

Research Article

Keywords: acute respiratory distress syndrome, bleomycin-induced lung injury, macrophage, molecular hydrogen, lung fibrosis

Posted Date: May 14th, 2021

DOI: https://doi.org/10.21203/rs.3.rs-504666/v1

Abstract

Background

Acute respiratory distress syndrome, which is caused by acute lung injury, is a destructive respiratory disorder caused by a systemic inflammatory response. Persistent inflammation results in irreversible alveolar fibrosis due to excessive activation of M2 macrophages. Because hydrogen gas possesses anti-inflammatory properties, we hypothesized that daily intermittent inhalation of hydrogen gas could suppress persist acute inflammation by inducing functional changes in macrophages, and consequently inhibit lung fibrosis during late-phase lung injury.

Methods

To test this hypothesis, lung injury was induced in mice by intratracheal administration of bleomycin (1.0 mg/kg). Mice were exposed to control gas (air) or hydrogen (3.2% in air) for 6 hours every day for 7 or 21 days. Respiratory physiology, tissue pathology, markers of inflammation, and macrophage phenotypes were examined.

Results

Mice with bleomycin-induced lung injury who received daily hydrogen therapy for 21 days (BH group) exhibited higher static compliance (0.056 mL/cmH_2O [95% CI:0.047–0.064] than mice with bleomycin-induced lung injury exposed only to air (BA group; 0.042 mL/cmH_2O [95% CI:0.031–0.053], p = 0.02) and lower static elastance (BH 18.8 cmH_2O/mL [95% CI:15.4–22.2] vs BA 26.7 cmH_2O/mL [95% CI:19.6–33.8], p = 0.02). When the mRNA levels of pro-inflammatory cytokines were examined 7 days after bleomycin administration, interleukin (IL)-6, IL-4 and IL-13 were significantly lower in the BH group than in the BA group. There were significantly fewer M2 macrophages in the alveolar interstitium of the BH group than in the BA group (3.1% [95% CI: 1.6%-4.5%] vs 1.1% [95% CI: 0.3%-1.8%], p = 0.008).

Conclusions

The results suggest that hydrogen inhalation inhibits the deterioration of respiratory physiological function and alveolar fibrosis in this model of acute lung injury by suppressing differentiation of M2 macrophages in the alveolar interstitium.

Introduction

Excessive, non-specific inflammation in the lungs initiates pathological processes leading to acute lung injury (ALI) and acute respiratory distress syndrome (ARDS), which directly and indirectly cause

destruction of lung tissue including alveolar structures [1]. The development of ALI/ARDS is triggered by an immune response that leads to activation of classically activated macrophages, or M1 macrophages, and accumulation of neutrophils in the alveoli. As a result, alveolar epithelial cells and vascular endothelial cells are extensively damaged, and pulmonary edema develops (exudation phase) [1, 2]. Seven to 10 days after onset, proliferation of type II alveolar epithelial cells and fibroblasts is observed in the destroyed alveoli (proliferative phase)[3]. This process of reconstruction is accompanied by persistent inflammation can promote alveolar fibrosis and decrease of alveolar compliance (fibrotic phase). Alternatively activated macrophages, or M2 macrophages, which differentiate as a result of persistent inflammation, play a key role in promoting disordered alveolar fibrosis [2]. Overexpression and persistence of M2 macrophages in the alveolar interstitium is a hallmark of the transition to the fibrotic phase [4, 5]. Therefore, novel therapies to reduce persistent inflammation prior to the establishment of irreversible alveolar fibrosis are required and have attracted great interest.

Molecular hydrogen has potent antioxidant and anti-inflammatory properties [6, 7]. The mechanisms underlying the anti-inflammatory effects of hydrogen are becoming clearer with known inhibition of proinflammatory cytokines and upstream signaling molecules [7–9]. Previous studies demonstrated that hydrogen ameliorates lung fibrosis caused by a variety of insults by inhibiting inflammatory signaling by the innate immune system and regulating signaling cascades that impact macrophages [8, 10, 11]. Inhalation of hydrogen gas may be a straightforward and promising therapeutic option, because inhaled gaseous molecules can directly reach the alveoli. Additionally, inhaled hydrogen has a low chemical toxicity [11–13]. Thus, this gaseous therapy has good clinical feasibility, as long as its flammability can be controlled.

A previous investigation demonstrated that hydrogen inhalation suppressed increases in oxidative stress and inflammation induced by intratracheal bleomycin administration in mice, and suppressed the malignant cycle toward lung fibrosis initiated by transforming growth factor (TGF)-β1 and inflammation [14]. This study was initially aimed to examine the hypothesis that hydrogen could reduce fibrosis in the ARDS fibrotic phase through suppression of lung inflammation and oxidative stress. However, Gao et al. reported hydrogen inhalation mitigated oxidative stress and reduced lung fibrosis using similar animal model after we initiated our experiments [14]. Therefore, to make the rationale of doing our experiment to fill the gap in knowledge, we tried to clarify the involved upstream mechanisms in the protective effects of hydrogen and focused on macrophage differentiation, which may be the target of hydrogen. Also, we tried to make a physiological assessment of the effects of hydrogen in clinically relevant evaluation using basal respiratory function parameters, since the protective effects of hydrogen were never physiologically tested in previous studies [7, 15]. Our results first showed that the primary effect of hydrogen was inhibition of inflammatory signaling in the innate immune system, which ameliorated lung fibrosis via regulation of signaling cascades that regulate M2 macrophage differentiation [8, 10, 16].

Materials And Methods

Animals

Eight-week-old, C57BL/6 male mice (21-23g, specific-pathogen free) were purchased from CLEA Japan Inc (Tokyo, Japan). Mice were kept on a 12-hour light / dark cycle at 20℃ to 22℃ and fed sterile food and water. Every effort was made to minimize the number of experimental animals and minimize pain or distress during the experimental procedures. All protocols followed the principles of laboratory animal care (NIH Publication No. 86-23, revised 1985), and all research protocols were reviewed and approved by the Animal Care and Use Committee, Okayama University (OKU-2018876). This study was conducted in compliance with the ARRIVE guidelines (https://arriveguidelines.org/). Animals were sacrificed at defined endpoints using CO_2 asphyxiation or by exsanguination under deep anesthesia with intraperitoneal administration of 0.75 mg / kg medetomidine hydrochloride (Domitor, Meiji Seika Pharma, Tokyo, Japan), 4 mg/kg midazolam (Dormicum, Astellas Pharma, Tokyo, Japan), and 5 mg/kg butorphanol (Vetorphale, Meiji Seika) as previously described [14]. Collected samples were snap-frozen using liquid nitrogen and stored at -80°C until use. Animals were checked twice daily after the administration of bleomycin. Dying animals were sacrificed using a humane endpoint.

Generation of ALI/ARDS with bleomycin administration and inhalation of hydrogen gas

This study was conducted using a well-established mouse model of ALI/ARDS and idiopathic pulmonary fibrosis [15, 17]. In summary, lung injury was generated by administrating bleomycin (bleomycin hydrochloride, Nippon Kayaku, Tokyo, Japan) dissolved in saline intratracheally via tracheotomy [18]. The bleomycin causes persistent inflammation pharmacologically in the bronchus and alveoli, eventually resulting in alveolar fibrosis. Mice were anesthetized, and an incision was made through the neck into the front of trachea. Bleomycin dissolved in saline (50 μl, 1 mg/kg) was injected using a Hamilton syringe and a 32G needle, then the wound was closed by cyanoacrylate glue. In sham controls, saline without bleomycin was administrated in the same manner. We conducted a preliminary pathologic assessment, which confirmed that bleomycin administration induced lung injury with temporal changes in pathology that mimicked those observed during ALI/ARDS (data not shown).

Mice were randomly assigned to 1 of 4 experimental groups: 1) saline administration and air inhalation (SA group), 2) saline administration and hydrogen inhalation (SH group), 3) bleomycin administration and air inhalation (BA group), and 4) bleomycin administration and hydrogen inhalation (BH group). A gas cylinder containing 4% hydrogen and 96% nitrogen blended gas was prepared (Taiyo Nissan, Tokyo, Japan). By mixing 800 mL/minute of the 4% H_2 /96% N_2 mixture and 200 mL/minute of 100% O_2 gas, a final mixture of 3.2% H_2, 20% O_2 and 76.8% N_2 gas, delivered at 1L / minute, was generated. Air for the control group is created by mixing 800 mL/minute of 100% N_2 gas and 200 ml/minute of 100% O_2 gas. For gas administration, 5 or fewer mice were placed in a sealed acrylic box (L 40 cm x W 20 cm x H 20 cm) for mixed gas exposure while temperature (acceptable range 22-24℃) and humidity (acceptable range 40-70%) were monitored. Mice were exposed to either air or 3.2% hydrogen in air for 6 hours every day for either 7 or 21 days.

Respiratory physiological examination

The respiratory physiology was evaluated using a FlexVent® small animal ventilator with spirometer (SCIREQ, Montreal, PQ, Canada). The programs for examination of respiratory function were already programmed into the device and were performed according to the manufacturer's instructions. Mice were anesthetized as described above, and 1 cm of a 18-gauge endotracheal tube was inserted into the trachea by tracheostomy. The endotracheal tube was attached to the FlexVent. Then, mechanical ventilation is started at 150 respirations per minute, 10 mL/kg of tidal volume, and an inspiratory:expiratory ratio of 2:3 for 1 minute. Inspiratory capacity (IC) was measured in mL using the "Deep Inflation" program where the lung was inflated with 27 cm H_2O of inspiratory pressure. The static compliance (Cst) in mL/cm H_2O and the static elastance (Est) in cm H_2O/mL were measured using the "PVs-V" program, where the lungs were inflated stepwise with 40 mL/kg of ventilation volume. Cst and Est were calculated by computer analysis according to the pressure-volume (PV) loop curve created. Total respiratory system resistance (Rs) was measured using the "SnapShot-150" program, where 3 repetitions of sine-wave-pressure forced ventilation (1.2 sec, 2.5 Hz) were performed. The protocol consisted of 1 minute of mechanical ventilation, 1 cycle of deep inflation, and three 1-minute cycles of mechanical ventilation using the Deep Inflation, the PVs-V, and finally the SnapShot-150 programs. IC, Cst and Est were calculated as the median of the three measurements.

Computed tomography

The lung computed tomography (CT) images were taken using a small-animal CT system, Latheta LCT200® (Hitachi, Ltd. Tokyo. JAPAN). The mice are sedated, then inserted into the CT machine and imaged with the following settings: Imaging condition, lung; Pixel size, 48 μm; Slice thickness, 192 μm; Slice interval, 192 μm; X-ray voltage, Low; Scale of tomographic image, -700 to +100; and Respiratory synchronization, "Yes". Of the 70 slices taken of the whole lung field, 40 slices in the center were used for analysis.

After the CT images were saved as JPG files, images of the inside of the thorax were extracted and converted to 8-bit grayscale. To trace the areas in the lung containing air, the the "Threshold" program was set at "Range: 0-136". To measure the area, the following settings in "Analyze Particles" program were used: Size (inch^2), 0 -Infinity; Circularity 0.00-1.00; and Show Bare Outline. The air-containing area of the whole lung field was calculated by integrating the slice width and the area containing air as detected above.

Hematoxylin and Eosin and Elastica Masson staining

The left upper lung lobes were fixed with 4% paraformaldehyde dissolved in phosphate buffered saline (PBS) for 2 days, embedded in paraffin, then sliced into 4-μm sections. Hematoxylin and eosin (HE) staining and Elastica Masson (E-M) staining were performed using standardized protocols by skilled technicians in the Central Research Laboratory at Okayama University. Images were automatically captured using the Nano-Zoomer 2.0RS slide scanner (Hamamatsu Photonics, Shizuoka, Japan) and analyzed using NDP.view2 software, (Hamamatsu Photonics, Shizuoka, Japan).

SYBR Green 2-step real-time reverse transcriptase polymerase chain reaction

Messenger RNA levels for interleukin (IL)-6, IL-4, IL-10, IL-13, collagen type I, fibronectin, and ribosomal protein L4 (RPL4) were assessed using SYBR Green, 2-step, real-time, reverse-transcription PCR. The whole right lungs were resected, frozen in liquid nitrogen, and ground into a powder. A portion of powdered lung tissue (30 mg) was used for RT-PCR. RNA extraction was performed with the Nucleospin® RNA kit (Takara Bio Inc., Kusatsu, Japan) according to the manufacturer's instruction. Total RNA (1 μg) was reverse transcribed with ReverTraAce® qPCR RT Master Mix (TOYOBO Inc., Osaka, Japan). The mixture for SYBR Green PCR was prepared using THUNDERBIRD SYBR qPCR MIX (TOYOBO Inc., Osaka, Japan) and primers (Supplementary information). The thermal cycling protocol activated the polymerase for 10 minutes at 95°C, followed by 40 cycles of 95°C for 15 seconds, and 60°C for 1 minute in a StepOnePlus Realtime PCR machine (Thermo Fisher Scientific, Waltham, Massachusetts).

Western blotting

Protein was extracted using radioimmunoprecipitation assay (RIPA) buffer, which consists of 50mM Tris-HCl (pH 8.0), 150mM NaCl,1 % Igepal® CA-630 (Merck, Darmstadt, Germany), 0.5 % Sodium deoxycshoate, 0.1 % sodium dodecyl sulfate (SDS) and 1mM EDTA, and cOmplete™ Mini Protease Inhibitor Cocktail (Merck. Darmstadt, Germany). Powdered frozen graft tissue (30 mg) was mixed with 300 μL of RIPA buffer, homogenized, and centrifuged. After measuring the protein concentration, samples were further dissolved in SDS-PAGE sample buffer (62.5 mM Tris-HCl pH 6.8, 10% glycerol, 2% SDS, bromophenol blue) to 1 μg/μL.

For the analysis of collagen type I (COL1), fibronectin and α-smooth muscle actin (αSMA), proteins (10μg) from lung tissue were separated by electrophoresis on 8% acrylamide gels without SDS and transferred to Immobilon®-P polyvinylidene difluoride (PVDF) membrane (0.45 μm) (Merck, Darmstadt, Germany). For the analysis of TGFβ, proteins (10μg) from lung tissue were separated by electrophoresis on 12% acrylamide, 0.1% SDS gels.

PVDF membranes are blocked with 5% non-fat dry milk to prevent non-specific binding of antibodies. Primary antibody against fibronectin, αSMA, COL1, and TGFβ were diluted with Can Get Signal immunoreaction enhancer solution 1 (Toyobo, Osaka, Japan) (Supplementary Information), and incubated with the membranes overnight at 4°C. Horseradish-peroxidase–conjugated secondary antibodies against mouse IgG and rabbit IgG were diluted with Can Get Signal immunoreaction enhancer solution 2 (Toyobo, Osaka, Japan) and membranes were incubated for 2 hours at room temperature. Chemiluminescence detection was performed with ECL Prime Western Blotting Detection Reagents (Cytiva, Tokyo, Japan) and a WSE-6100 LuminoGraph I (ATTO Corporation, Tokyo, Japan).

Immunohistochemistry

Paraffin-embedded lung tissue sections (4 μm) were immunostained for TGF-β using an ABC Kit (Vector laboratories INC., Burlingame, California). Information on the primary and secondary antibodies used is

shown in the Supplementary Information. Sections were deparaffinized, rehydrated, and treated for antigen retrieval with 10 mM citric acid pH 6.0 at 120°C for 10 minutes in a pressure cooker. Endogenous peroxidase inhibition was performed with 0.3% hydrogen peroxide in PBS for 20 minutes at room temperature. Blocking treatment was performed with 10% goat serum in tris buffered saline with 0.1% Tween 20 (TBS-T) to prevent non-specific binding of antibodies. The primary antibodies were diluted by Can Get Signal immunostaining Solution A (Toyobo, Osaka, Japan), applied to the sections, incubated overnight at 4°C, and then washed with TBS-T. Biotin-conjugated secondary antibodies were diluted by Can Get Signal immunostaining Solution A, applied on the sections, and incubated for 2 hours at room temperature. After washing, ABC reagent was applied to the sections then incubated for 30 minutes at room temperature as per the manufacturer's instructions. For 3,3'-diaminobenzidine (DAB) staining, one DAB tablet was dissolved in 50 mL of 0.05mol/l Tris-HCl buffer pH 7.6 with 10 µL of 30% hydrogen peroxide as per the manufacturer's instructions. Sections were incubated in DAB solution for 10 minutes at room temperature, then washed under running water, counterstained with hematoxylin, dehydration, clearing, and coverslipping

Immunofluorescence

Paraffin blocks were sectioned, deparaffinized, dehydrated, and treated for antigen retrieval using the technique described above. The multiplex fluorescent immunostaining was used for staining with anti-ionized calcium binding adaptor molecule 1 (Iba-1) antibody and anti-CD163 antibody. Information on primary and secondary antibodies is given in the Supplementary Information. Blocking treatment was performed with Super Block® (SCY AAA125, Cosmo Bio Co., Ltd. Tokyo, Japan). Anti-Iba-1 antibody and anti-CD163 antibody were diluted in Can Get Signal immunostaining Solution A, then incubated on the tissue section overnight at 4°C. After washing, the sections were incubated with fluorescently labeled secondary antibodies with Alexa Flour (AF) 488 or 594. DAPI-Fluoromount G® (0100-20, SouthernBiotech, Birmingham, AL) was used for nuclear staining and sealing.

Fluorescent images were taken by the Mantra^{TM} Quantitative Pathology Imaging System (PerkinElmer Inc., Waltham, Massachusetts), and cells were counted in the alveoli and interstitium were automatically using the InForm® 2.4.10 software (Akoya Biosciences, Inc., Menlo Park, California). Three images were taken randomly from each section with a 200x image. Fluorescence imaging was performed at 488 nm, and 594 nm wavelengths. In the InForm software, a computer learning system was used to learn the characteristics of alveolar epithelium and alveolar interstitum tissues and exclude tracheal epithelial cells. The cells were identified by DAPI staining, and the immunostaining was visualized at 488 nm (Iba-1) or 594 nm (CD163) wavelength. The intensity thresholds for Iba-1-positive and CD163-positive cells were carefully adjusted and identified, and all images were analyzed according to the same rules. The median of the 3 results obtained for each section was then analyzed.

Statistics

Statistical analysis was performed using IBM SPSS Statistics version 23.0 (IBM, Armonk, New York). Statistically significant differences between groups were determined using the Kruskal-Wallis test followed by Dunn's multiple comparison test. All values are presented as mean ± 95% confidence interval (CI). Results were considered significant at $P < 0.05$.

Results

Hydrogen inhalation mitigates respiratory physiological dysfunction during fibrotic phase after bleomycin-induced lung injury.

To determine the impact of hydrogen inhalation on respiratory function, several basal parameters were examined after lung injury with bleomycin and 21 days of hydrogen inhalation or sham/ air therapy. While IC and Rs were not significantly different between mice that received hydrogen therapy and mice that received sham/ air therapy (BH group vs BA group, Fig. 1a, b), Cst, an index of the distensibility of the respiratory system, was significantly higher in mice that received hydrogen therapy (BH 0.056 mL/cm H_2O [95% CI: 0.47–0.64] vs BA 0.042 mL/cm H_2O [95% CI: 0.031–0.053], p = 0.02)(Fig. 1c). The Est of the lungs in mice that received hydrogen therapy after lung injury was significantly lower than in mice with air therapy (BH 18.8 cm H_2O/mL [95% CI: 15.4–22.2] vs BA 26.7 cm H_2O/mL [95% CI: 19.6–33.8], p = 0.02) (Fig. 1d). In fibrotic phase after lung injury, fibrotic changes progress in the alveolar interstitum, and the lung tissues become hardened. These results suggests that hydrogen inhalation therapy preserved the ability of the lung to expand and reduced lung stiffness. There were no differences in any of the respiratory parameters examined between hydrogen and sham/ air therapy when lung injury was not induced (SH and SA groups), suggesting that hydrogen has no effects on respiratory physiological function in individuals without alveolar damage (Fig. 1).

Hydrogen inhalation can attenuate the reduction in lung capacity typical of bleomycin-induced lung injury.

After lung injury and 21 days of hydrogen therapy or sham/ air therapy, lung capacity was measured directly using CT volumetry (Fig. 2a, left column). The aerated area in each CT section was identified (Fig. 2a, right column), quantitated, and used to calculate the volume of aerated space in lung (Fig. 2b). Although bleomycin-induced lung injury significantly reduced aerated lung capacity (BA group), hydrogen treatment partially ameliorated this reduction, and the BH group had higher aerated lung capacity than the BA group (BH 296μL [95% CI: 245–347] vs BA 207μL [95% CI: 128–286], p = 0.02). Hydrogen treatment had no effect on aerated lung capacity in the absence of lung injury (SH and SA groups) (Fig. 2b).

Hydrogen reduced alveolar fibrosis in fibrotic phase after bleomycin-induced lung injury.

Histopathological evaluation for fibrosis was performed 21 days after lung injury. There were many cytoplasm-rich cells, which might include fibroblasts, myofibroblasts, and inflammatory cells, in the alveolar interstitium in lungs with bleomycin-induced ALI. The presence of these cells in the alveolar

interstitium was attenuated by hydrogen treatment (BH group) (Fig. 3, H&E staining). Collagen bundles were seen in the interstitium of the mice with bleomycin-induced ALI (BA group) and were less frequently observed in mice treated with hydrogen (BH group)(Fig. 3, E-M).

Hydrogen inhibited increases in fibronectin protein expression during fibrotic phase after bleomycin-induced lung injury.

When the expression of extracellular matrix proteins was examined after bleomycin-induced ALI, expression of COL1 and αSMA did not differ between any of the treatment groups. (Fig. 4a). Fibronectin was more highly expressed after bleomycin-induced ALI in the BA group than SA group (BA 0.371 [95% CI: 0.314–0.428] vs SA 0.212 [95% CI: 0.143–0.281], p = 0.004), and hydrogen therapy showed a tendency to reduce this upregulation, though the differences in protein levels did not reach statistical significance (BH 0.294 [95% CI: 0.245–0.343] vs BA 0.371 [95% CI: 0.314–0.428], p = 0.069) (Fig. 4b).

Hydrogen inhalation attenuates the upregulation of critical interleukins and downregulates fibronectin mRNA in lung tissue early after bleomycin-induced lung injury.

IL-6 is a cytokine produced by alveolar endothelial cells and macrophages in response to the innate immune system and is a major mediator of fever and acute reactions. IL-6 also promotes the differentiation of type 2 T helper cells, which produce IL-4, IL-13 and L-10, and M2 macrophages [19–22]. IL-4 and IL-13 are signals that induce monocytes to differentiate into M2 macrophages [23–25]. IL-10 are signals that suppresses the expression of pro-inflammatory cytokines. Expression of the mRNAs for IL-6, IL-4 and IL-13, all of which are considered pro-inflammatory cytokines in the lung, were significantly upregulated 7 days after bleomycin administration to induce ALI as compared with saline-treated control lungs. Intermittent hydrogen inhalation significantly suppressed upregulation of IL-6, IL-4 and IL-13 in response to bleomycin-induced ALI (Fig. 5a, b, and c). The bleomycin-induced expression of IL-10 tended to be lower after hydrogen therapy; however, this difference did not reach statistical significance (BH 0.437 [95% CI: 0.374–0.499] vs BA 0.683 [95% CI: 0.474–0.891], p = 0.13).

The mRNA expression of fibrinogen and COL1, components of the extracellular matrix, were also investigated 7 days after bleomycin treatment. The levels of fibrinogen mRNA were reduced by hydrogen therapy, while the levels of COL1 mRNA were not. These results mirrored the protein expression levels seen 21 days after bleomycin treatment (Fig. 4).

Hydrogen inhalation suppresses the expression of TGF-β in the alveolar interstitium early after bleomycin-induced lung injury.

TGF-β1 is secreted by many cell types, including macrophages [26]. Because TGF-β1 plays a central role in fibrosis by inducing epithelial cells, vascular endothelial cells, and mesenchymal cells to adopt a phenotype that produces extracellular matrix proteins, we examined TGF-β1 expression after bleomycin-induced ALI and changes in expression in response to hydrogen therapy. In western blot analysis, the 44 kDa band is likely the latent form of TGF-β1, while the 13 kDa band is the active form. When TGF-β1

protein expression was analyzed by Western blotting, hydrogen treatment did not affect TGF-β1 expression (Fig. 6a). However, when the localization of TGF-β1 was examined using immunostaining, fewer TGF-β1-positive cells were found in the alveolar interstitium after hydrogen therapy than in sham/air treated controls (Fig. 6b).

Hydrogen inhalation reduces M2 macrophages in the alveolar interstitium after bleomycin-induced lung injury.

Because IL-4 and IL-13 are known to drive the differentiation of M2 macrophages and hydrogen therapy mitigated increases in IL-4 and IL-13 expression that typically accompany bleomycin-induced ALI, we performed immunofluorescent staining identify the phenotype of macrophages in the alveoli and alveolar interstitum in the 4 treatment groups. Anti-Iba-1 antibody was used to detect all macrophages, anti-CD163 antibody was used to specifically detect M2 macrophages, and the number of macrophages by phenotype was measured. Bleomycin-induced ALI increased the number of Iba-1-positive, CD163-negative macrophages in the alveoli, and hydrogen treatment had no effect on the number of Iba-1-positive, CD163-negative cells present (BA 13.0% [95% CI: 9.3%-16.8%] vs BH 11.5% [95% CI: 7.8%-15.1%], p = 0.74) (Fig. 7b). Bleomycin-induced ALI also increased the number of Iba-1-positive, CD163-positive macrophages in the alveoli, indicating that more M2 macrophages were present in the tissue. Hydrogen therapy significantly decreased the presence of these M2 macrophages in the alveoli (BA 3.1% [95% CI: 1.6%-4.5%] vs BH 1.1% [95% CI: 0.3%-1.8%], p = 0.008) (Fig. 7c). These results suggest that one mechanism whereby hydrogen inhalation preserves lung function is blocking the differentiation of macrophages.

Discussion

Hydrogen inhalation therapy has been proven effective in mitigating in several animal models of lung injury including hyperoxic lung injury, hemorrhagic shock-induced lung injury, radiation-induced lung injury, and bronchial asthma [5, 7, 8, 27]. Our study is the first to prove that hydrogen inhalation therapy effectively attenuates the decline of respiratory physiological function induced by bleomycin in a mouse model of persistent lung inflammation and fibrosis. We also demonstrated that the protective effects of hydrogen gas inhalation therapy in this lung injury model were accompanied by, and like due in part to, attenuation of pro-inflammatory cytokine expression and inhibition of M2 macrophage differentiation. Identifying macrophage differentiation as a potential underlying mechanism of hydrogen therapy advances our understanding of hydrogen biology.

In this study, we administered an air mixture with 3.2% hydrogen concentration for 6 hours daily beginning in the day of bleomycin administration to induce ALI and continuing for 21 days. Other investigations of inhaled hydrogen therapy have shown effective results with hydrogen concentrations of 2–4% [7, 26–31]. Intermittent inhalation was reported to be more effective than continuous inhalation in rat model of Parkinson's disease [1]. Because the endpoint of this study was to assess lung function during fibrotic phase after lung injury, we targeted treatment to the proliferative phase of ALI/ARDS, which

ordinary occurs 7 to 21 days after the onset of lung injury [1]. Our preliminary studies indicated that the bleomycin-induced lung injury model mimicked the temporal changes in pathology observed during ALI/ARDS and dictated our protocol of intermittent hydrogen inhalation for 21 days after bleomycin administration.

During ALI/ARDS, pathogen-associated molecular pattern molecules and damage-associated molecular pattern molecules stimulate type II alveolar epithelial cells and alveolar macrophages to secrete pro-inflammatory cytokines. The permeability of pulmonary capillaries and alveolar epithelial cells increases, and exudate flows from the blood vessels into alveoli and its interstitium. The immune cells responsible for this are classically activated macrophages (M1 macrophages) and neutrophils [32]. Innate immune sensors, such as Toll-like receptors (TLRs), are expressed not only on macrophages but also on type II alveolar epithelial cells [33]. TLRs sense inflammatory signals, resulting in the recruitment of the adaptor protein myeloid differentiation factor 88 (MyD88), and ultimately in nuclear migration of nuclear factor κB (NF-κB), which binds to its recognition sites in DNA and activates transcription of pro-inflammatory cytokines, such as IL-6 and tumor necrosis factor-α [34]. IL-6, which is expressed in type II alveolar epithelial cells and M1 macrophages, is associated with lung fibrosis through the differentiation of M2 macrophages [19–23]. Although M2 macrophages are important for tissue repair, an excess of M2 macrophages can cause organ fibrosis [25, 34]. Suppression or deletion of IL-6 suppresses M2 macrophage differentiation and attenuates lung fibrosis [35, 36]. Our finding that hydrogen inhalation therapy reduced IL-6 mRNA expression is consistent with published work demonstrating that hydrogen suppresses the expression of IL-6 [7, 23, 27, 37–42]. Therefore, it is reasonable to hypothesize that the reduction in IL-6 expression in response to hydrogen inhalation therapy caused less M2 macrophage differentiation and less fibrosis after bleomycin-induced ALI.

IL-4 and IL-13 also induce the differentiation of macrophages to M2 macrophages, which decreases inflammation and encourages tissue repair. Persistent or excessive expression of IL-4 or IL-13 and the accompanying M2 macrophage differentiation leads to abnormal organ fibrosis [24, 25]. In our study, the expression of IL-4, and IL-13 mRNAs were decreased by hydrogen inhalation therapy. The regulation of IL-4 and IL-13 by hydrogen may result in an anti-fibrotic effect through suppression of M2 macrophage differentiation and thereby reduce alveolar fibrosis. TGF-β is secreted from M2 macrophages. Hydrogen administration decreased the number of TGF-β-producing cells in the alveolar interstitium, again indicating that control of M2 macrophage differentiation may be an important mechanism underlying the therapeutic benefits of inhaled hydrogen. The results of this study support models put forth by others that hydrogen therapy regulates upstream signals in a cascade impacting macrophages and innate immunity that leads to inflammation [7, 8, 10, 43].

A previous study using a bleomycin-induced ALI model was reported by Gao and colleagues who found that hydrogen attenuated oxidative stress, increased the expression of the antioxidant glutathione peroxidase, and consequently suppressed the expression of reactive oxygen species in the injured lung [13]. The expression of TGF-β1 was also suppressed and epithelial-to-mesenchymal transition was inhibited, which may be one mechanisms involved in fibrosis suppression by hydrogen treatment. In our

study, there was no change in TGF-β1 protein expression in the lungs, however there were fewer TGF-β1-expressing cells in the alveolar interstitium after hydrogen therapy.

Our study adds several novel findings to the published literature on therapeutic hydrogen in animal models of lung injury. Importantly, we found that hydrogen inhalation suppressed the expression of IL-4 and IL-13 in the lungs in the bleomycin-induced ALI model and suppressed the appearance of M2 macrophages in the alveolar interstitium, likely by suppressing their differentiation. These mechanisms are associated with suppression of lung fibrosis late after ALI. Another unique aspect of this study was that the degree of preservation of lung function after hydrogen treatment was formally examined using physiological respiratory function tests and CT volumetry. Hydrogen administration increased ventilation and increased alveolar compliance, which strongly suggested that hydrogen inhalation would improve the clinical profile of ALI/ARDS patients when used as therapy.

The study has some limitations. The pathogenesis of ALI/ARDS in clinical practice is diverse. Bleomycin-induced lung injury is only one type of drug-induced lung injury and does not replicate all possible ALI/ARDS presentations. Determining the most effective hydrogen administration regimen will require additional study and was not a focus of these experiments. Finally, the mechanisms by which hydrogen inhibits the expression of cytokines (IL-6, IL-4, IL-13) were not analyzed. These will need to be clarified in future studies.

Conclusion

Intermittent hydrogen inhalation therapy with 3.2% hydrogen for 6 hours per day for 21 days inhibited the decline of respiratory physiological function and increase in alveolar fibrosis typical of ALI. This inhibition of ALI was partially due to via suppression of differentiation of M2 macrophages in the alveolar interstitium in this mouse model of bleomycin-induced ALI.

List Of Abbreviations

BA, bleomycin administration and air inhalation; BH, bleomycin administration and hydrogen inhalation; SA, saline administration and air inhalation; SH, saline administration and hydrogen inhalation; IC, Inspiratory capacity; Cst, static compliance; Est, static elastance; Rs, respiratory system resistance; E-M, elastica Masson; RPL4, ribosomal protein L4; COL1, collagen type I; αSMA, α-smooth muscle actin; Iba-1, ionized calcium binding adaptor molecule 1;

Declarations

Ethics approval and consent to participate

The ethics approval was obtained from the Animal Care and Use Committee, Okayama University (OKU-2018876).

Consent for publication

Not applicable.

Availability of data and materials

The datasets used and/or analyzed during the current study are available from the corresponding author on reasonable request.

Competing interests

The authors declare no conflicts of interest.

Funding

This study was supported by a grant from the JSPS KAKENHI, Grant Number 19K09416, and Teijin Pharma Limited, Grant Number TJNS20190415006.

Authors' contributions

TA: Participated in the research design, research performance, data acquisition, data interpretation, and data analysis and wrote the manuscript; TH, TN and MS: Participated in performing the research; YT: Instructed the technique of creating bleomycin intratracheal administration model; MIk: Instructed the technique of immunofluorescence, interpretation of results, and Involved in statistical processing; MIs: Participated in performing the histopathological data analysis; AT and NMi: Instructed on the technique of conducting respiratory physiology tests and involved in interpretation of the results; AN: Provided the working hypothesis, contributed to the study design, and was involved in revising the article for intellectual content; IO and HN: Provided the working hypothesis, participated in the research design, performance of the research, and data acquisition, and wrote the manuscript and supervised the entire research procedure and analysis; All authors reviewed and approved the final manuscript.

Acknowledgements

We thank Toshiyuki Ishiwata (Tokyo Metropolitan Institute of Gerontology, Tokyo, Japan) for provision and technical guidance using the Mantra System and InForm software. We thank Shannon Wyszomierski, PhD for editing the manuscript.

Supplementary information

Supplementary information is available at BMC Pulmonary Medicine's website.

Additional file 1: Primer and antibody summery.

References

1. Thompson BT, Drazen JM, Chambers RC, Liu KD. Acute Respiratory Distress Syndrome. New England Journal of Medicine 2017; 377:562–572.
2. Chen X, Tang J, Shuai W, Meng J, Feng J, Han Z. Macrophage polarization and its role in the pathogenesis of acute lung injury/acute respiratory distress syndrome. Inflamm Res 2020; 69:883–895.
3. Gordon S. Alternative activation of macrophages. Nat Rev Immunol 2003; 3:23–35.
4. Duru N, Wolfson B, Zhou Q. Mechanisms of the alternative activation of macrophages and non-coding RNAs in the development of radiation-induced lung fibrosis. World J Biol Chem 2016; 7:231–239.
5. Ohsawa I, Ishikawa M, Takahashi K, Watanabe M, Nishimaki K, Yamagata K et al. Hydrogen acts as a therapeutic antioxidant by selectively reducing cytotoxic oxygen radicals. Nature Medicine 2007; 13:688–694.
6. Fukuda K, Asoh S, Ishikawa M, Yamamoto Y, Ohsawa I, Ohta S. Inhalation of hydrogen gas suppresses hepatic injury caused by ischemia/reperfusion through reducing oxidative stress. Biochem Biophys Res Commun 2007; 361:670–674.
7. Kawamura T, Wakabayashi N, Shigemura N, Huang C-S, Masutani K, Tanaka Y et al. Hydrogen gas reduces hyperoxic lung injury via the Nrf2 pathway in vivo. American Journal of Physiology-Lung Cellular and Molecular Physiology 2013; 304:L646-L656.
8. Huang P, Wei S, Huang W, Wu P, Chen S, Tao A et al. Hydrogen gas inhalation enhances alveolar macrophage phagocytosis in an ovalbumin-induced asthma model. Int Immunopharmacol 2019; 74:105646.
9. Xie K, Zhang Y, Wang Y, Meng X, Wang Y, Yu Y et al. Hydrogen attenuates sepsis-associated encephalopathy by NRF2 mediated NLRP3 pathway inactivation. Inflamm Res 2020; 69:697–710.
10. Itoh T, Hamada N, Terazawa R, Ito M, Ohno K, Ichihara M et al. Molecular hydrogen inhibits lipopolysaccharide/interferon γ-induced nitric oxide production through modulation of signal transduction in macrophages. Biochem Biophys Res Commun 2011; 411:143–149.
11. National Aeronautics and Space Administration, Safety Standard for Hydrogen and Hydrogen Systems: Guidelines for Hydrogen System Design, Materials Selection, Operations, Storage and Transportation. 1997. https://ntrs.nasa.gov/citations/19970033338. Accessed 18 April 2021.
12. Abraini JH, Gardette-Chauffour MC, Martinez E, Rostain JC, Lemaire C. Psychophysiological reactions in humans during an open sea dive to 500 m with a hydrogen-helium-oxygen mixture. J Appl Physiol (1985) 1994; 76:1113–1118.
13. Gao L, Jiang D, Geng J, Dong R, Dai H. Hydrogen inhalation attenuated bleomycin-induced pulmonary fibrosis by inhibiting transforming growth factor-β1 and relevant oxidative stress and epithelial-to-mesenchymal transition. Experimental Physiology 2019; 104:1942–1951.
14. Matute-Bello G, Frevert CW, Martin TR. Animal models of acute lung injury. Am J Physiol Lung Cell Mol Physiol 2008; 295:L379-399.

15. Izbicki G, Segel MJ, Christensen TG, Conner MW, Breuer R. Time course of bleomycin-induced lung fibrosis. Int J Exp Pathol 2002; 83:111–119.
16. Kawai S, Takagi Y, Kaneko S, Kurosawa T. Effect of three types of mixed anesthetic agents alternate to ketamine in mice. Exp Anim 2011; 60:481–487.
17. Terasaki Y, Fukuda Y, Ishizaki M, Yamanaka N. Increased expression of epimorphin in bleomycin-induced pulmonary fibrosis in mice. Am J Respir Cell Mol Biol 2000; 23:168–174.
18. Travis MA, Sheppard D. TGF-beta activation and function in immunity. Annu Rev Immunol 2014; 32:51–82.
19. Diehl S, Rincón M. The two faces of IL-6 on Th1/Th2 differentiation. Molecular Immunology 2002; 39:531–536.
20. Epstein Shochet G, Brook E, Bardenstein-Wald B, Shitrit D. TGF-beta pathway activation by idiopathic pulmonary fibrosis (IPF) fibroblast derived soluble factors is mediated by IL-6 trans-signaling. Respir Res 2020; 21:56.
21. Fujimoto M, Serada S, Mihara M, Uchiyama Y, Yoshida H, Koike N et al. Interleukin-6 blockade suppresses autoimmune arthritis in mice by the inhibition of inflammatory Th17 responses. Arthritis Rheum 2008; 58:3710–3719.
22. Hashimoto-Kataoka T, Hosen N, Sonobe T, Arita Y, Yasui T, Masaki T et al. Interleukin-6/interleukin-21 signaling axis is critical in the pathogenesis of pulmonary arterial hypertension. Proc Natl Acad Sci U S A 2015; 112:E2677-2686.
23. Wynn TA. Fibrotic disease and the T(H)1/T(H)2 paradigm. Nat Rev Immunol 2004; 4:583–594.
24. Novak ML, Koh TJ. Macrophage phenotypes during tissue repair. J Leukoc Biol 2013; 93:875–881.
25. Bosurgi L, Cao YG, Cabeza-Cabrerizo M, Tucci A, Hughes LD, Kong Y et al. Macrophage function in tissue repair and remodeling requires IL-4 or IL-13 with apoptotic cells. Science 2017; 356:1072–1076.
26. Terasaki Y, Ohsawa I, Terasaki M, Takahashi M, Kunugi S, Dedong K et al. Hydrogen therapy attenuates irradiation-induced lung damage by reducing oxidative stress. Am J Physiol Lung Cell Mol Physiol 2011; 301:L415-426.
27. Kohama K, Yamashita H, Aoyama-Ishikawa M, Takahashi T, Billiar TR, Nishimura T et al. Hydrogen inhalation protects against acute lung injury induced by hemorrhagic shock and resuscitation. Surgery 2015; 158:399–407.
28. Hayashida K, Sano M, Kamimura N, Yokota T, Suzuki M, Ohta S et al. Hydrogen inhalation during normoxic resuscitation improves neurological outcome in a rat model of cardiac arrest independently of targeted temperature management. Circulation 2014; 130:2173–2180.
29. Hayashida K, Sano M, Ohsawa I, Shinmura K, Tamaki K, Kimura K et al. Inhalation of hydrogen gas reduces infarct size in the rat model of myocardial ischemia-reperfusion injury. Biochem Biophys Res Commun 2008; 373:30–35.

30. Kawamura T, Huang CS, Peng X, Masutani K, Shigemura N, Billiar TR et al. The effect of donor treatment with hydrogen on lung allograft function in rats. Surgery 2011; 150:240–249.
31. Ito M, Hirayama M, Yamai K, Goto S, Ito M, Ichihara M et al. Drinking hydrogen water and intermittent hydrogen gas exposure, but not lactulose or continuous hydrogen gas exposure, prevent 6-hydorxydopamine-induced Parkinson's disease in rats. Med Gas Res 2012; 2:15.
32. Crestani B, Cornillet P, Dehoux M, Rolland C, Guenounou M, Aubier M. Alveolar type II epithelial cells produce interleukin-6 in vitro and in vivo. Regulation by alveolar macrophage secretory products. J Clin Invest 1994; 94:731–740.
33. Imai Y, Kuba K, Neely GG, Yaghubian-Malhami R, Perkmann T, van Loo G et al. Identification of oxidative stress and Toll-like receptor 4 signaling as a key pathway of acute lung injury. Cell 2008; 133:235–249.
34. Saito F, Tasaka S, Inoue K, Miyamoto K, Nakano Y, Ogawa Y et al. Role of interleukin-6 in bleomycin-induced lung inflammatory changes in mice. Am J Respir Cell Mol Biol 2008; 38:566–571.
35. Mauer J, Chaurasia B, Goldau J, Vogt MC, Ruud J, Nguyen KD et al. Signaling by IL-6 promotes alternative activation of macrophages to limit endotoxemia and obesity-associated resistance to insulin. Nat Immunol 2014; 15:423–430.
36. Cardinal JS, Zhan J, Wang Y, Sugimoto R, Tsung A, McCurry KR et al. Oral hydrogen water prevents chronic allograft nephropathy in rats. Kidney Int 2010; 77:101–109.
37. Fujii Y, Shirai M, Inamori S, Shimouchi A, Sonobe T, Tsuchimochi H et al. Insufflation of hydrogen gas restrains the inflammatory response of cardiopulmonary bypass in a rat model. Artif Organs 2013; 37:136–141.
38. Liu W, Shan LP, Dong XS, Liu XW, Ma T, Liu Z. Combined early fluid resuscitation and hydrogen inhalation attenuates lung and intestine injury. World J Gastroenterol 2013; 19:492–502.
39. Gu H, Yang M, Zhao X, Zhao B, Sun X, Gao X. Pretreatment with hydrogen-rich saline reduces the damage caused by glycerol-induced rhabdomyolysis and acute kidney injury in rats. Journal of Surgical Research 2014; 188:243–249.
40. Shimosawa T, Guo SX, Jin YY, Fang Q, You CG, Wang XG et al. Beneficial Effects of Hydrogen-Rich Saline on Early Burn-Wound Progression in Rats. Plos One 2015; 10.
41. Zhai Y, Zhou X, Dai Q, Fan Y, Huang X. Hydrogen-rich saline ameliorates lung injury associated with cecal ligation and puncture-induced sepsis in rats. Exp Mol Pathol 2015; 98:268–276.
42. Iketani M, Ohshiro J, Urushibara T, Takahashi M, Arai T, Kawaguchi H et al. Preadministration of Hydrogen-Rich Water Protects Against Lipopolysaccharide-Induced Sepsis and Attenuates Liver Injury. Shock 2017; 48:85–93.
43. Liu GD, Zhang H, Wang L, Han Q, Zhou SF, Liu P. Molecular hydrogen regulates the expression of miR-9, miR-21 and miR-199 in LPS-activated retinal microglia cells. Int J Ophthalmol 2013; 6:280–285.

Figures

Fig 1

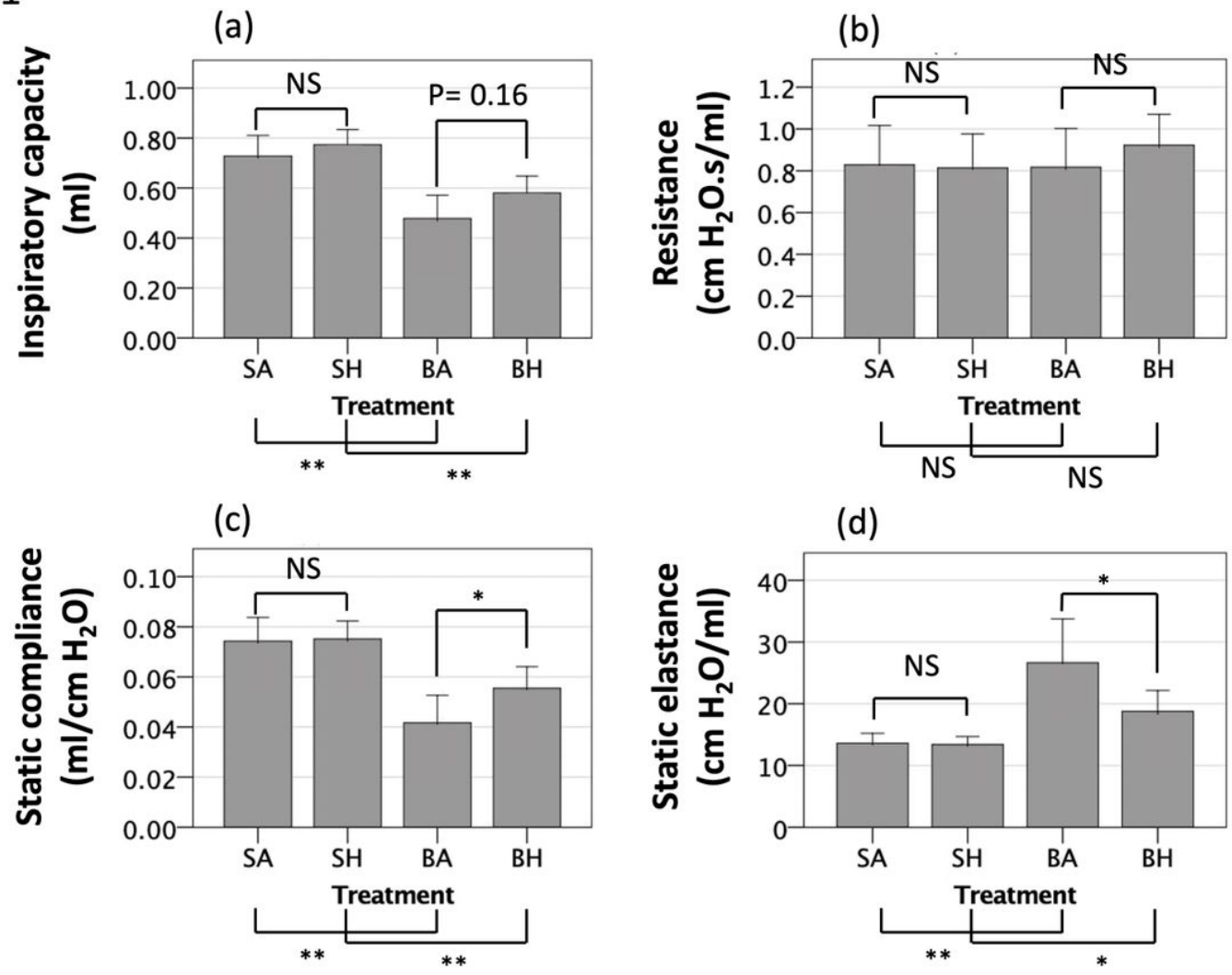

Figure 1

The results of respiratory physiological examination of respiratory function during the fibrotic phase of bleomycin-induced lung injury. (a) Inspiratory capacity (IC). (b) Total respiratory system resistance (Rs). There were no differences in Rs among the four groups (p=0.51). (c) Static compliance (Cst). (d) Static elastance (Est). The BA and BH groups had lower IC and Cst and higher Est than the SA and SH groups; the BH group had significantly higher Cst and lower Est than the BA group. SA, saline administration and air inhalation, n=6; SH, saline administration and hydrogen inhalation, n=6; BA, bleomycin administration and air inhalation, n=11; BH, bleomycin administration and hydrogen inhalation, n=11. NS, not significant; *, $p < 0.05$; **, $p < 0.01$; error bars indicate 95% CI.

Fig 2

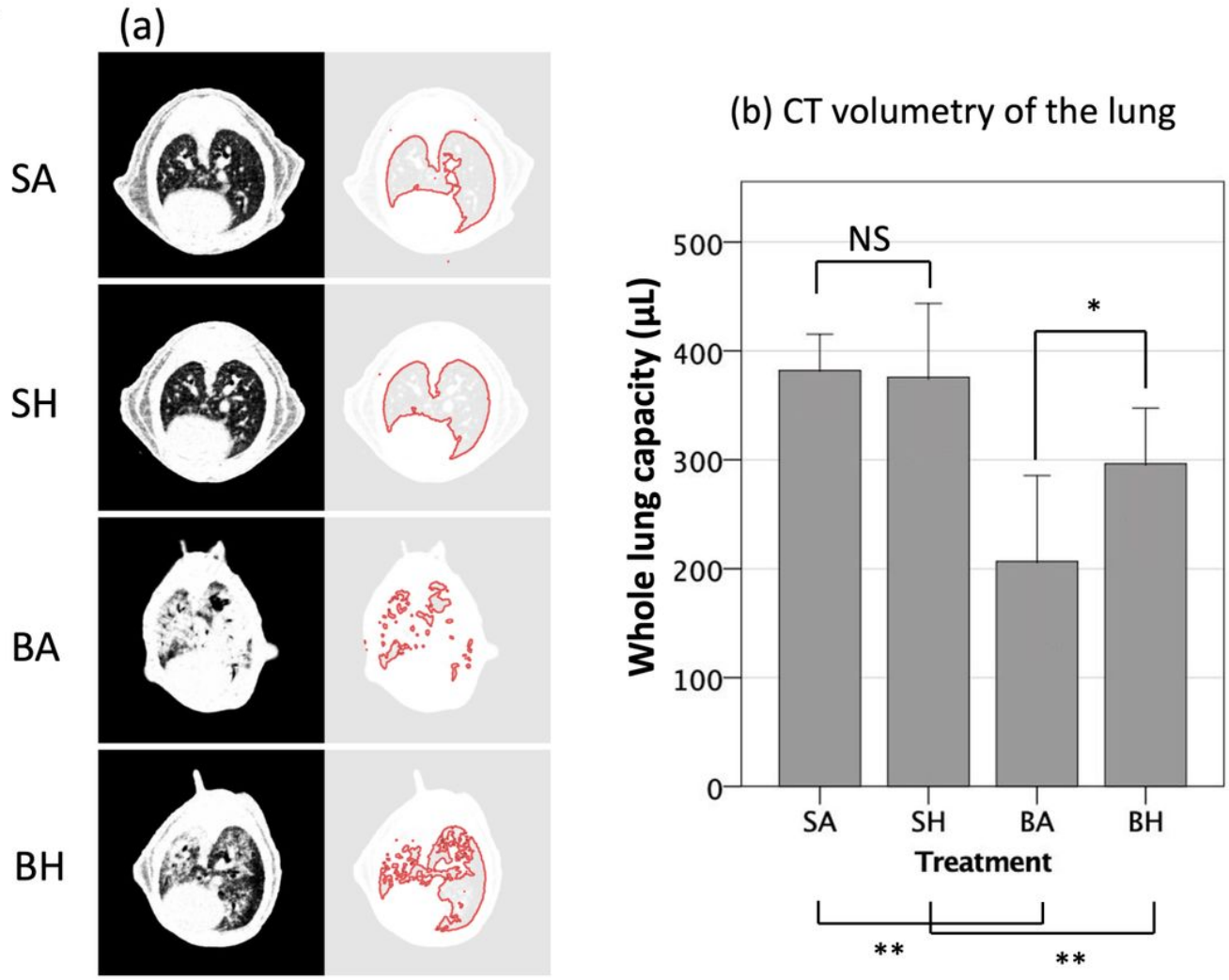

Figure 2

Volumetry evaluated using computed tomography. (a) Left Column. CT images of the thoracic cavity at the level of the left ventricle. Right Column. Representative images obtained using "Analyze Particles" program. The "Bare Outline" is indicated by the red line. The area of the aerated field, that enclosed within the red lines, was analyzed with ImageJ. (b) The aerated volume was calculated by integrating the aerated area. The aerated volume was reduced by bleomycin-induced lung injury, and inhaling hydrogen preserved the aerated volume after bleomycin-induced injury. SA, saline administration and air inhalation, n=4; SH, saline administration and hydrogen inhalation, n=4; BA, bleomycin administration and air inhalation, n=7, BH, bleomycin administration and hydrogen inhalation, n=6. NS, not significant; *$p < 0.05$, **$p < 0.01$. Error bars: 95% CI.

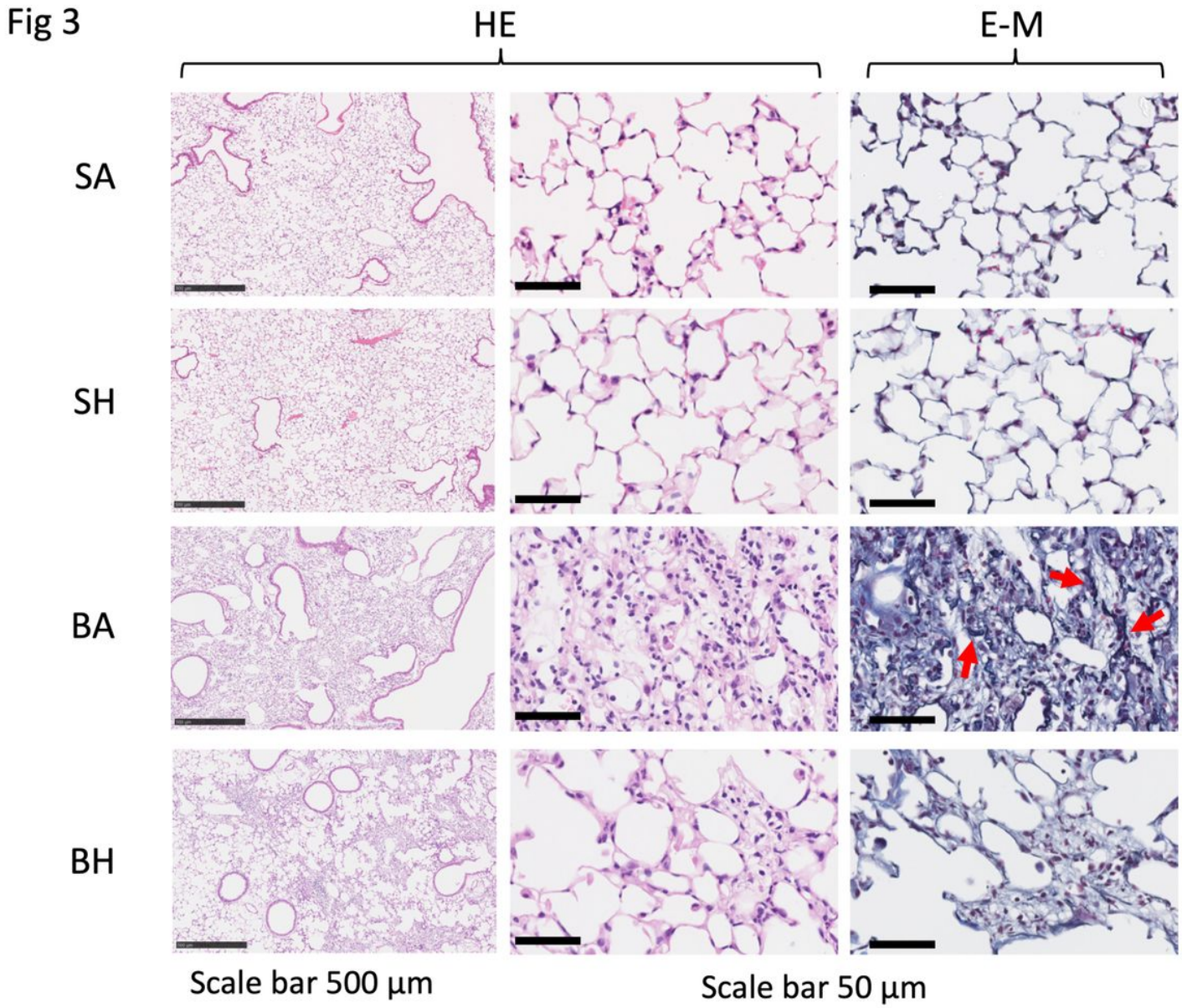

Figure 3

Examination of alveolar fibrosis in left upper lobe lung tissue. Representative images of bleomycin-induced alternations in the alveolar interstitum and bronchial epithelium are shown using hematoxylin and eosin (HE) staining (12.5x and 200x images) and Elastica Masson (E-M) staining (200x image). Extracellular matrix component proteins appear as blue-purple in E-M staining. Red arrows indicated particularly thick collagen bundles, which stain as black-purple bundles. Inhalation of hydrogen gas suppressed fibrous tissue production after lung injury.

Fig 4

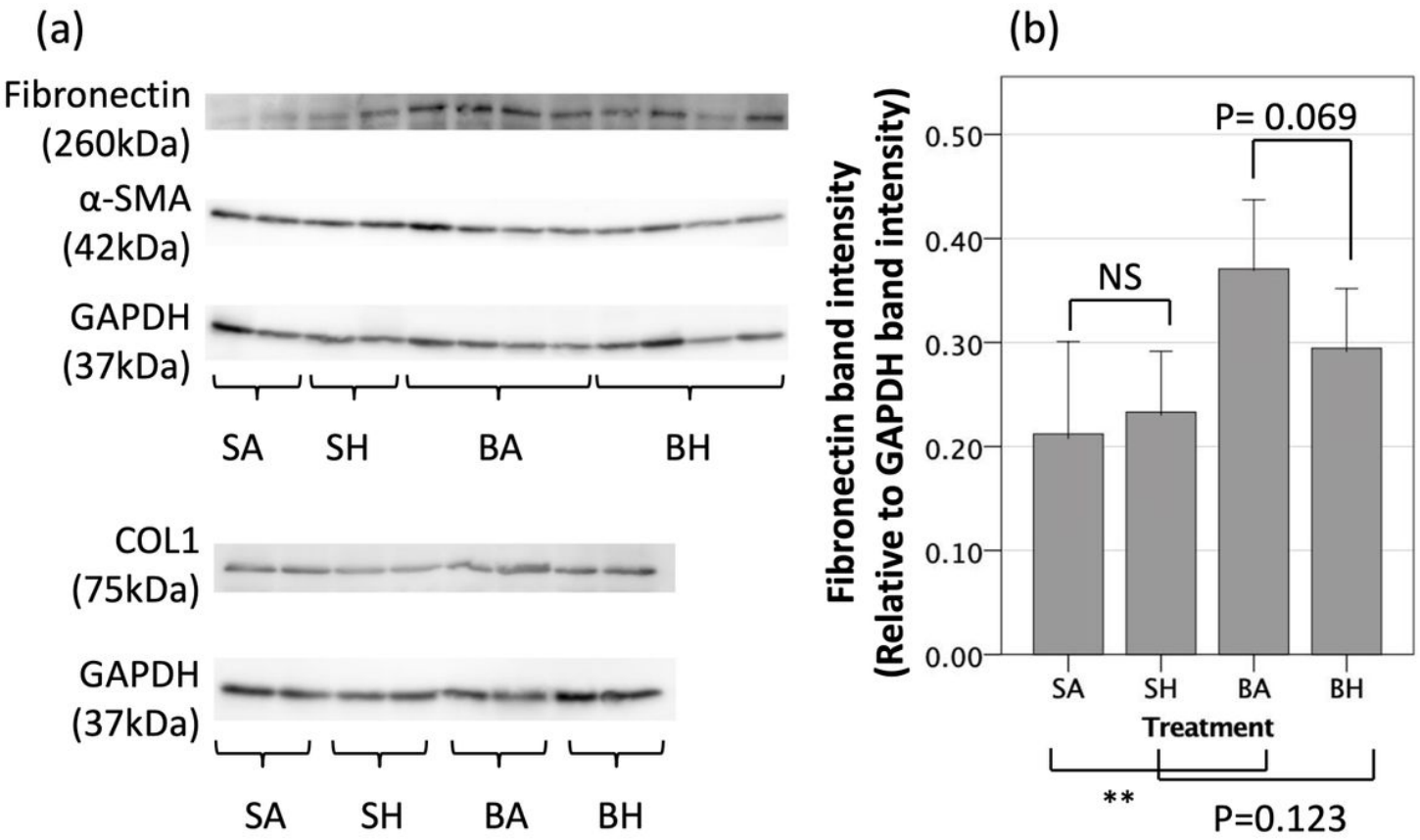

Figure 4

Western blot evaluation of extracellular matrix component proteins. (a) Western blot evaluation of fibronectin, type 1 collagen (COL1), alpha-smooth muscle actin (αSMA) and glyceraldehyde 3-phosphate dehydrogenase (GAPDH). (b) The band intensity of fibronectin evaluated as a ratio to GAPDH. Inhaling hydrogen gas may decrease the production of fibronectin in lung (p=0.069). SA, saline administration and air inhalation, n=6; SH, saline administration and hydrogen inhalation, n=6; BA, bleomycin administration and air inhalation, n=11, BH, bleomycin administration and hydrogen inhalation, n=11. NS: not significant, **p < 0.01. Error bars: 95% CI.

Fig 5

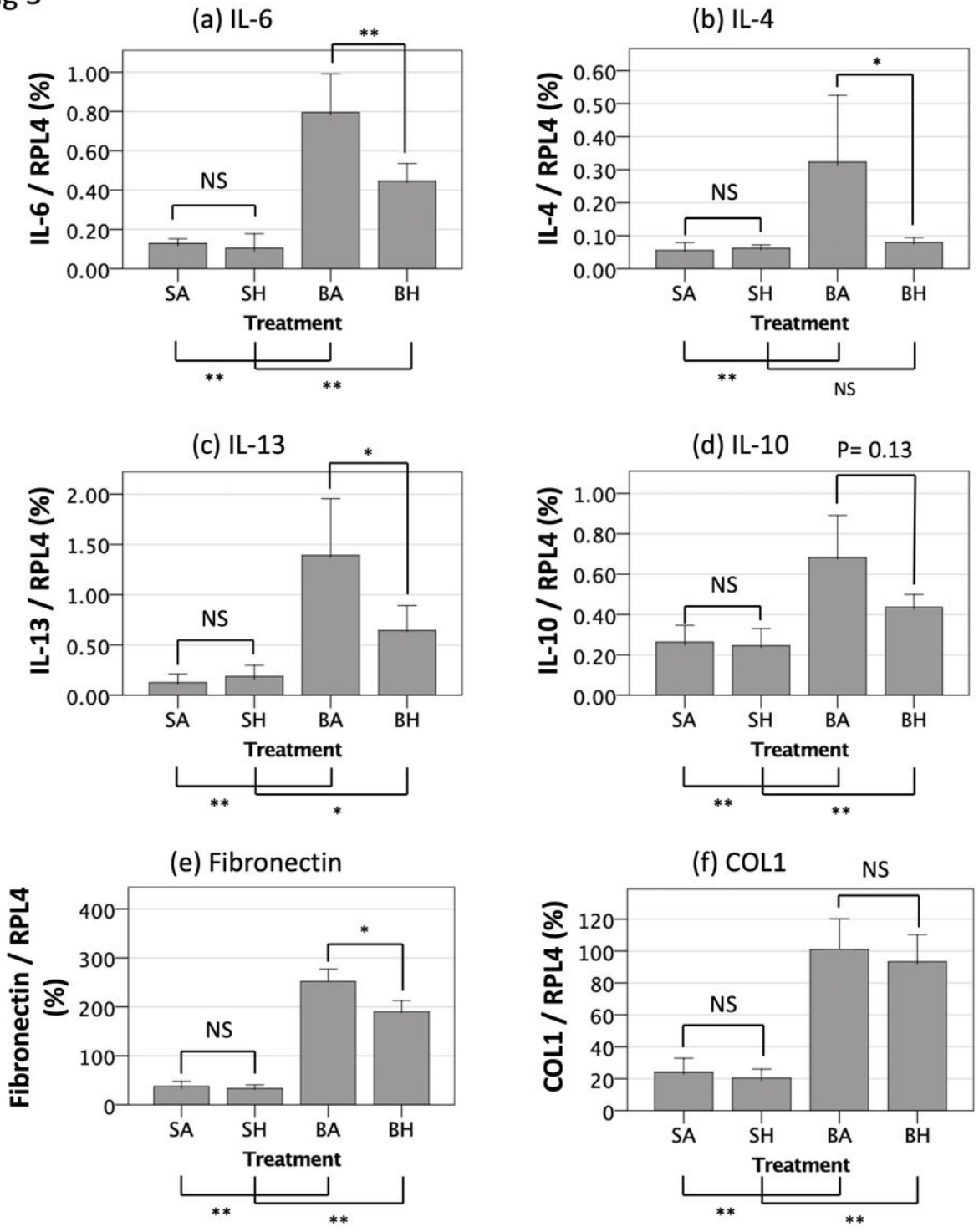

Figure 5

mRNA expression levels of (a) interleukin (IL)-6, (b) IL-4, (c) IL-13, (d) IL-10, (e) fibronectin and (f) type 1 collagen (COL1) were measured using SYBR Green 2-step real-time reverse transcriptase polymerase chain reaction (RT-PCR). Inhaling hydrogen gas significantly suppressed the expression of IL-6, IL-4, and IL-13 induced by bleomycin administration. The expression of fibronectin is significantly reduced by hydrogen inhalation. SA, saline administration and air inhalation, n=12; SH, saline administration and

hydrogen inhalation, n=12; BA, bleomycin administration and air inhalation, n=32, BH, bleomycin administration and hydrogen inhalation, n=34. NS: not significant, *p < 0.05, **p < 0.01. Error bars: 95% CI.

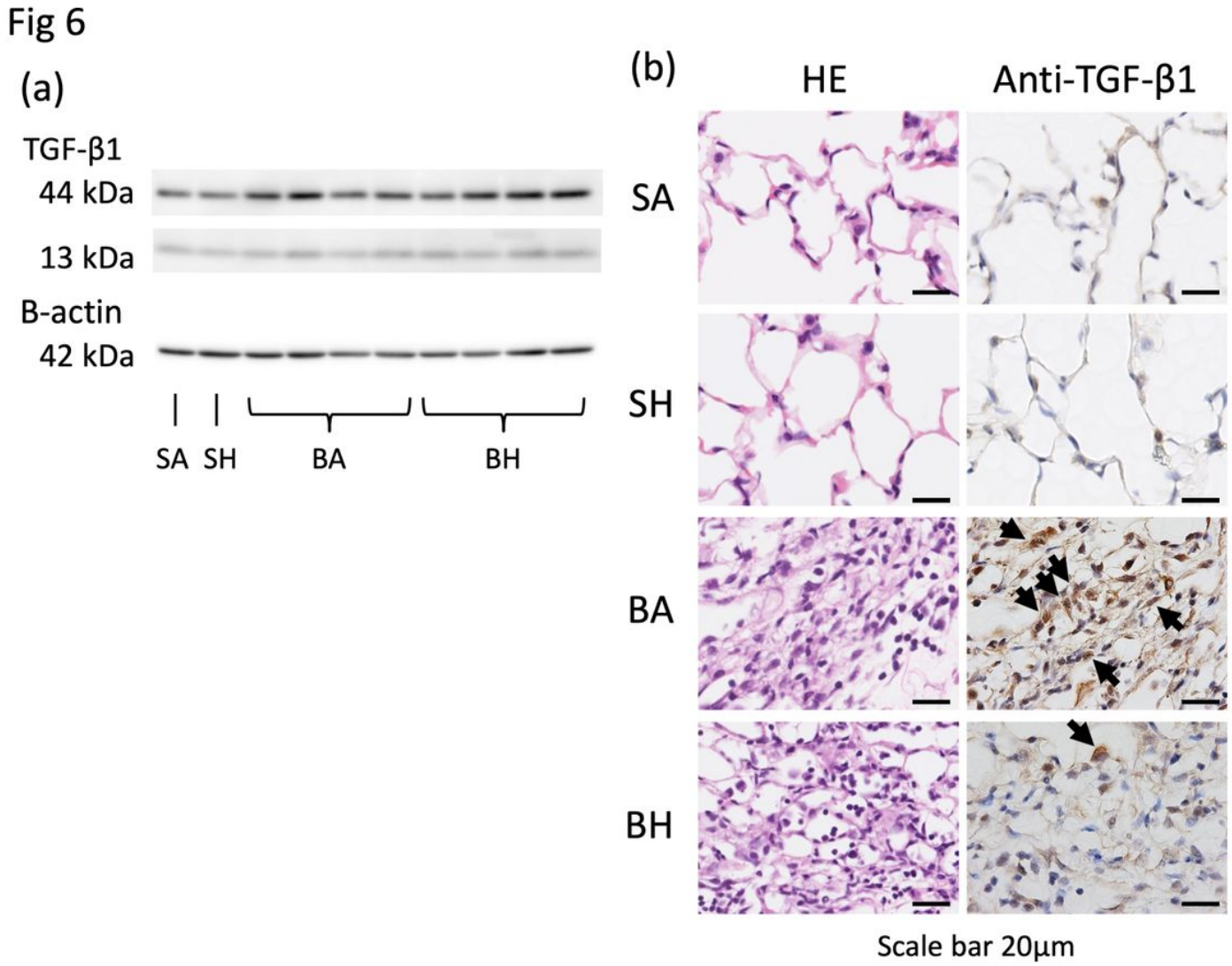

Figure 6

TGF-β1 expression. (a) TGF-β1 protein in the lung as examined by western blotting. Beta-actin was evaluated as a housekeeping protein. There are two TGF-β1 bands, 44kDa and 13kDa. The 13kDa band represents active form. There was no difference of 13 kDa band intensity among the 4 groups. (b) Immunostaining for TGF-β1 to localize protein expression in the alveoli. Black arrows indicate cells strongly positive for TGF-β1. SA, saline administration and air inhalation; SH, saline administration and hydrogen inhalation; BA, bleomycin administration and air inhalation; BH, bleomycin administration and hydrogen inhalation.

Fig 7

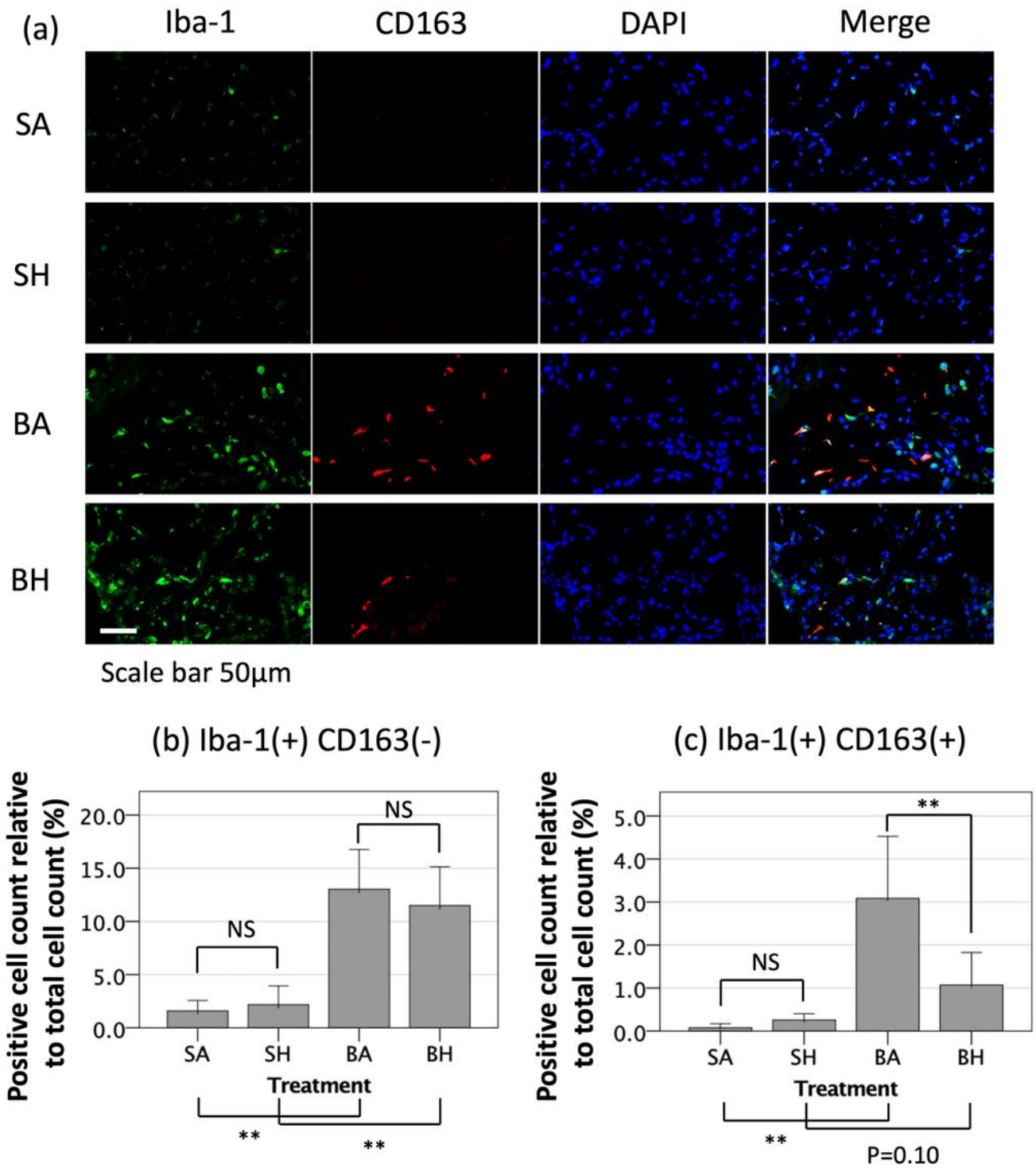

Figure 7

Immunofluorescent localization of macrophage markers. (a) Anti-Iba-1 was used to detect total macrophages, and anti-CD163 was used to detect M2 macrophages. Representative images showing DAPI (blue), Iba-1 (Green, AlexaFlour488), and CD 163 (red, AlexaFlour594). (b) Quantitation of Iba-1-positive, CD163-negative cells (all macrophages except M2 macrophages). (c) Quantitation of Iba-1-positive, CD163-positive cells (M2 macrophages). The graphs show the percentage obtained by dividing

the number of macrophages of the target phenotype by the total number of cells (measured by DAPI staining). There was no difference in the number of Iba-1-positive and CD163-negative cells between the groups with and without hydrogen inhalation; however, the number of Iba-1-positive and CD163-positive cells was significantly reduced by inhaling hydrogen. SA, saline administration and air inhalation, n=6; SH, saline administration and hydrogen inhalation, n=6; BA, bleomycin administration and air inhalation, n=15, BH, bleomycin administration and hydrogen inhalation, n=15. NS: not significant, *p < 0.05, **p < 0.01. Error bars: 95% CI.

Supplementary Files

This is a list of supplementary files associated with this preprint. Click to download.

- SupplementaryFile.docx